Universiteit
Leiden
The Netherlands

Upconverting nanovesicles for the activation of ruthenium anti-cancer prodrugs with red light

Askes, S.H.C.

Citation
Askes, S. H. C. (2016, November 24). *Upconverting nanovesicles for the activation of ruthenium anti-cancer prodrugs with red light*. Retrieved from https://hdl.handle.net/1887/44378

Version:	Not Applicable (or Unknown)
License:	Licence agreement concerning inclusion of doctoral thesis in the Institutional Repository of the University of Leiden
Downloaded from:	https://hdl.handle.net/1887/44378

Note: To cite this publication please use the final published version (if applicable).

Cover Page

Universiteit Leiden

The handle http://hdl.handle.net/1887/44378 holds various files of this Leiden University dissertation.

Author: Askes, S.H.C.
Title: Converting nanovesicles for the activation of ruthenium anti-cancer prodrugs with red light
Issue Date: 2016-11-24

CHAPTER 7

Synthesis and in-vitro application of upconverting silica-coated liposomes

Light upconversion by triplet-triplet annihilation (TTA-UC) in nanoparticles has received considerable research attention for bio-imaging and light activation of prodrugs. However, the mechanism of TTA-UC is inherently sensitive for quenching by molecular oxygen. A potential oxygen protection strategy is the coating of TTA-UC nanoparticles with a layer of oxygen impermeable material. In this work, we explore if (organo)silica can fulfill this role. Three synthesis routes are described for obtaining monodispersed (organo)silica-coated red-to-blue upconverting liposomes; their upconversion properties are investigated in solution and in A549 lung carcinoma cells. Although it was found that the silica offered no protection from oxygen in solution and after uptake in A549 cancer cells, upon drying of the silica-coated liposome dispersion in an excess of (organo)silica precursor, interesting liposome-silica nanocomposite materials were obtained that were capable of generating light upconversion in air.

Sven H. C. Askes, Vincent Leeuwenburgh, Wim Pomp, Stefania Grecea, Thomas Schmidt, and Sylvestre Bonnet. Manuscript in preparation.

7.1 Introduction

Photon upconversion is defined as the generation of high energy light (*e.g.* blue) from low energy light (*e.g.* red). Among the wide variety of applications, light upconversion has received substantial interest in upconversion bio-imaging and as method to shift the activation wavelength of photoactivatable anticancer prodrugs towards the phototherapeutic window.[1] One mechanism of light upconversion is triplet-triplet annihilation upconversion (TTA-UC), which is based on the photophysical interplay of photosensitizer and annihilator chromophores (see Chapter 2, Figure 2.1).[2] The photosensitizer absorbs low energy light, after which a long lived triplet excited state is reached *via* intersystem crossing. The energy of this triplet state is transferred to the annihilator upon diffusional collision by means of triplet-triplet energy transfer (TTET); a succession of TTET leads to a buildup of long lived triplet state annihilators. Two triplet state annihilators can then perform triplet-triplet annihilation upconversion, in which one of them departs with all the energy and reaches a high energy singlet excited state. Finally, this singlet excited state returns to the ground state by fluorescent emission of a high energy photon, realizing light upconversion. TTA-UC has been demonstrated in an extensive assortment of organic, inorganic, and/or supramolecular materials,[3] as well as in nano- or micro-sized particles,[4] and has been used for applications in photocatalysis,[5] solar energy harvesting,[6] drug delivery and activation,[1a, 1b] and bio-imaging.[7]

Evidently, for biological application of TTA-UC, supramolecular assemblies are required to co-localize photosensitizer and annihilator. Furthermore, for the biological application in anticancer applications, such an assembly is required to support efficient TTA-UC, have selective uptake in tumors, and cause minimal toxicity for healthy tissues. Meanwhile, liposomes functionalized with PEGylated lipids have emerged since decades as supramolecular tools in drug delivery. Liposomes have high biocompatibility and low toxicity, and accumulate selectively in tumors because of the enhanced permeability and retention effect (EPR).[8] Our group recently combined liposomes with TTA-UC: red-to-blue upconversion was demonstrated in the lipid bilayer of neutral PEGylated DMPC (1,2-dimyristoyl-*sn*-glycero-3-phosphocholine) liposomes.[1a, 1b] These upconverting liposomes were further functionalized with a blue-light activatable Ru(II) polypyridyl complex. Upon red light irradiation of this combined system, the upconverted light was efficiently transferred to the Ru-complex *via* FRET, which triggered the release of the photoactivated

compound. This mechanism may be exploited in photoactivated cancer therapy to release a cytotoxic compound in tumors.

However, no upconversion could be observed in air, because molecular oxygen quenches the triplet states of sensitizer and annihilator. In other words, the upconverting drug carrier did not function in oxygen-rich conditions, and the use of this system *in vitro* would lead to unreliable performance, because oxygen concentrations vary drastically in the complex microenvironment of a tumor.[9] Oxygen sensitivity can be reduced by developing upconversion systems that either (i) feature very fast TTA UC so that upconversion takes place on a shorter timescale than physical quenching by molecular oxygen, (ii) have built-in functionality for the consumption of molecular oxygen to create a locally oxygen-depleted microenvironment, or (iii) are protected by a nanoscale oxygen-impenetrable barrier. Most noteworthy examples of the latter strategy include upconverting oil-core nanocapsules embedded in an oxygen protective cellulose material or polyvinyl alcohol nanofibers,[3f, 10] and upconversion in hyperbrached unsaturated polyphosphoesters.[11] However, there are no examples yet where a nanoscale oxygen-barrier is used to protect TTA-UC in a drug delivery system. In this work, we attempt to coat upconverting liposomes with (organo)silica[I] as potential oxygen barrier and investigate the oxygen protection potential of such a silica barrier.

Using silica has several advantages. First of all, silica has been widely recognized as a chemically inert, biocompatible, *pH* insensitive, and transparent material.[12] Secondly, the silica surface can be modified to attach molecules such as PEG, biotin, or Ru(II)-complexes.[13] Finally, it has been demonstrated that nm-thick silica layers can act as an oxygen barrier in silica-coated polymer films,[14] and it has been suggested that silica protects oxygen-sensitive chromophores such as $[Ru(bpy)_3]^{2+}$ and $[Ru(phen)_3]^{2+}$ in doped silica nanoparticles.[15] Silica-coating of liposomes has been described before;[16] for example, Bégu *et al*. described the application of a silica-coating to DPPC liposomes (1,2-dipalmitoyl-*sn*-glycero-3-phosphocholine) by sequential hydrolysis and condensation of tetraethylorthosilicate (TEOS) as silica precursor.[16a, 16b, 17] It was suggested that the deposition of silica on the membrane was controlled by hydrogen-bonding interactions between the

[I] Organosilica is defined as silica containing organic groups as integral part of its structure

phosphate groups of the lipids, interfacial water, and silanol groups of the silica. Furthermore, nitrogen adsorption isotherms suggested that the dried particles were non-porous. However, most of the published articles do not explicitly discuss whether the particles are stable and monodispersed in aqueous buffer, which is a important criterion for a drug delivery device.

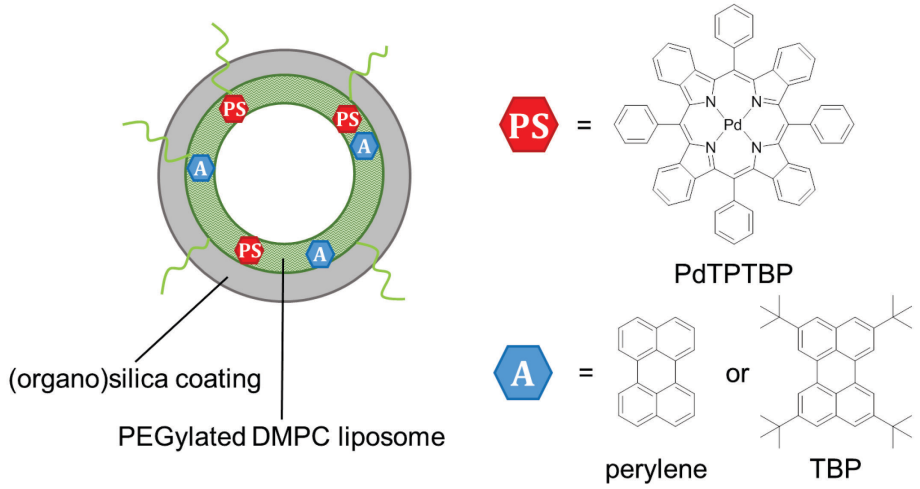

*Figure 7.1. Schematic representation of (organo)silica-coated liposomes containing photosensitizer (PS; PdTPTBP) and annihilator chromophores (A; perylene or TBP). PdTPTBP = palladium tetraphenyltetrabenzoporphyrin, TBP = 3,5,8,11-tetra(*tert*-butyl)perylene*

This chapter describes three synthetic routes for obtaining monodispersed (organo)silica-coated DMPC liposomes containing a red-to-blue upconverting couple, *i.e.* palladium tetraphenyltetrabenzoporphyrin (PdTPTBP) and perylene (Figure 7.1). In a second step, the upconverting properties of silica-coated liposomes are investigated in order to assess whether silica can act as an oxygen-barrier to allow upconversion in air. Furthermore, the uptake of these particles and their ability to perform upconversion *in vitro* will be evaluated. Finally, the silica-coated liposomes are dried in presence of an excess of (organo)silica precursor and the upconversion properties of the resulting nanocomposite materials are investigated.

7.2 Results and Discussion

7.2.1 Preparation of upconverting liposomes

Preliminary attempts to reproduce the work of Bégu *et al.*, who described the synthesis of silica-coated liposomes based on direct addition of tetraethylorthosilicate (TEOS) to non-PEGylated DPPC liposomes were

unsuccessful.[16b] In our hands, these experiments inevitably led to the formation of silica nanoparticles, gelation of the reaction mixture, and/or aggregation of the silica-coated liposomes. Also, silica-coating experiments with 1,2-dilauroyl-sn-glycero-3-phosphocholine (DLPC) liposomes were unsuccessful. Therefore, only DMPC-based liposomes were further considered for preparing silica-coated liposomes. Three synthetic routes, called methods A, B, and C, were developed to apply an (organo)silica-coating to upconverting DMPC liposomes and obtain monodispersed particles (Figure 7.2).

First of all, upconverting DMPC liposomes (from now on called **UL**) were prepared according to a literature procedure.[1a] Briefly, a mixture of 5 mM 1,2-dimyristoyl-sn-glycero-3-phosphocholine (DMPC), 4 mol% sodium N-(carbonyl-methoxypolyethylene glycol-2000)-1,2-distearoyl-*sn*-glycero-3-phosphoethanolamine (DSPE-mPEG-2000) was used to prepare liposomes *via* a hydration-extrusion method in phosphate buffered saline (PBS). A red-to-blue upconverting TTA-UC couple was selected for incorporation in the liposomes, consisting of palladium(II) tetraphenyltetrabenzoporphyrin (PdTPTBP, 0.05 mol%) and perylene (0.5 mol%). Dynamic light scattering (DLS) measurements reported a reproducible average hydrodynamic diameter (z-ave) of around 150 nm and a polydispersity index (PDI) of 0.1 (Table 7.1). The UV-vis absorption spectrum (Figure 7.3) of **UL** shows the characteristic absorption peaks of perylene (390, 414, 440 nm) and PdTPTBP (440, 630 nm). The emission spectrum (λ_{exc} = 630 nm, 80 mW.cm^{-2}) of **UL** in 50 mM sodium sulfite in PBS shows both the phosphorescence of PdTPTBP and the perylene-based emission, characteristic of upconversion with this dye couple (Figure 7.3a).[1a] In Figure 7.3b, the temperature dependence is shown of the upconversion emission and phosphorescence. The upconversion first increases up to 25 °C, and then decreases slightly, while the phosphorescence decreases steeply up to 25 °C, and then continues to decrease, but less steeply. The rise in upconversion up to 25 °C is explained by the fact that the DMPC membrane changes its phase from gel to liquid crystalline at 24 °C;[18] in the liquid crystalline phase the fluidity of the membrane is increased, and collision-dependent processes such as TTET and TTA become more efficient.[1a] A detailed discussion of this phenomenon is described in Chapter 6. Here, this thermo-photophysical phenomenon is used to verify the integrity of the lipid bilayer after silica-coating (see below).

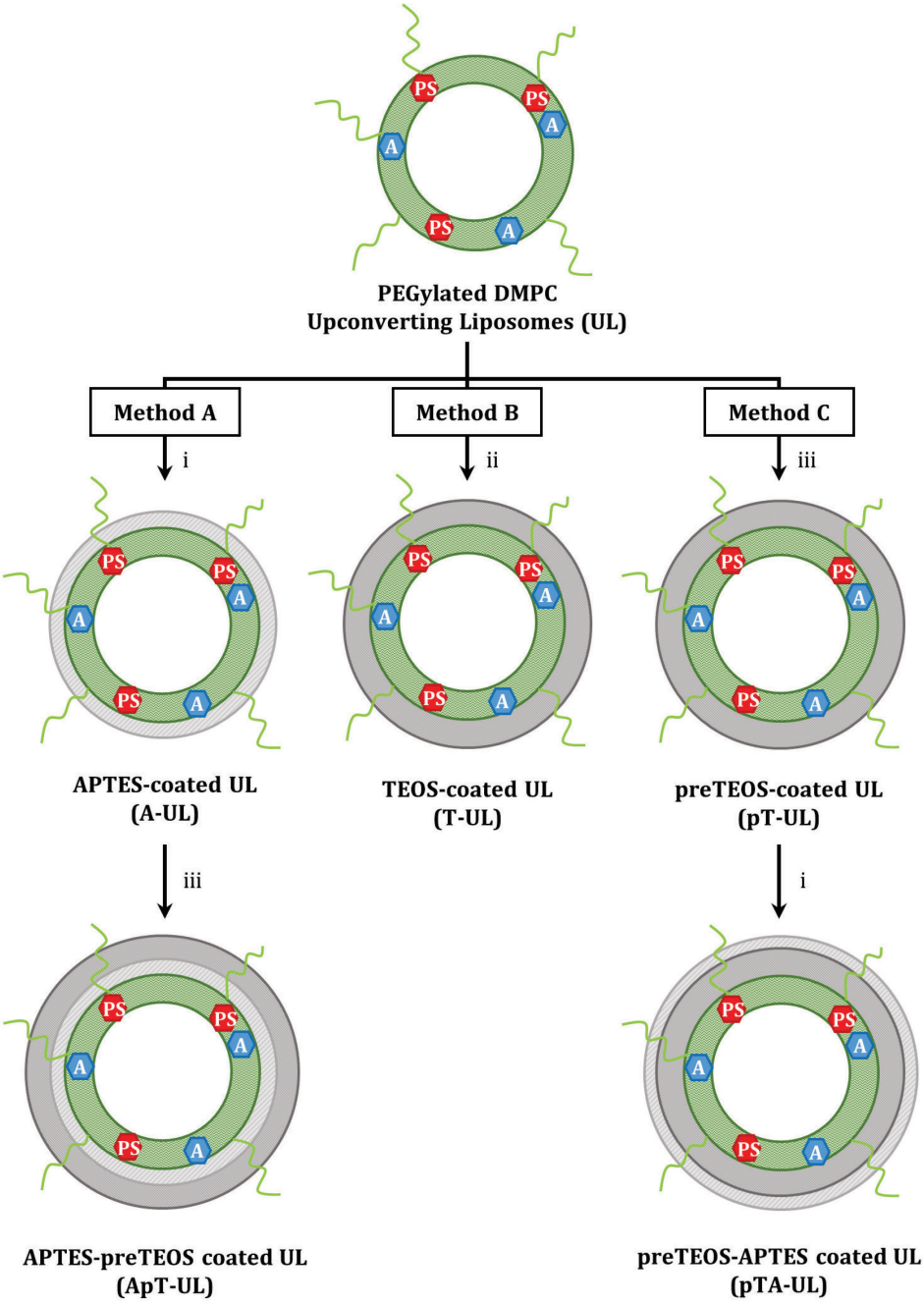

Figure 7.2. Three different synthesis methods to obtain silica-coated upconverting PEGylated liposomes. Conditions per eq. DMPC: (i) 25 eq. APTES, 16 h; (ii) 8 eq. TEOS, 1 M HCl, 30 min (iii) 8 eq. "preTEOS" (TEOS, stirred for 24 h in PBS (50 mM) at 40 °C before addition), 24 h.

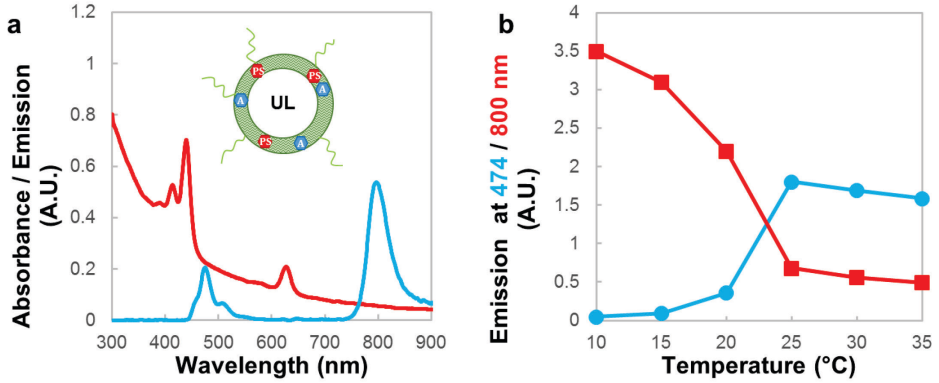

*Figure 7.3. a) Absorption spectrum (red) and emission spectrum (blue) of **UL** under 10 mW 630 nm irradiation (80 mW.cm^{-2}) at 20 °C in 50 mM Na_2SO_3 PBS in air. b) Temperature dependency of upconversion (at 474 nm) and phosphorescence (at 800 nm) of **UL** in 50 mM Na_2SO_3 PBS in air.*

*Table 7.1. Physical characterization of liposomes **UL** and (organo)silica-coated liposomes **A-UL**, **pT-UL**, **pTA-UL**, **ApT-UL** and **T-UL** by Dynamic Light Scattering (DLS) and zeta-potentiometry, with reported average hydrodynamic diameter (z-ave), polydispersity index (PDI) and zeta potential at the given pH.*

Sample	z-ave (nm)[a]	PDI[a]	zeta potential[b] (mV)	*pH*
UL	148 ± 4	0.09 ± 0.01	−16 ± 0	7.1
A-UL (unwashed)	171 ± 5	0.14 ± 0.02		
A-UL	128 ± 1	0.10 ± 0.02	−40 ± 5	6.8
ApT-UL	145 ± 1	0.15 ± 0.01	−20 ± 0	7.0
pT-UL			−19 ± 1	6.9
pTA-UL	167 ± 1	0.15 ± 0.01	−17 ± 1	7.2
T-UL			−33 ± 1	6.7

[a] Standard deviation based on N ≥ 3 samples. [b] Standard deviation based on 3 measurements of the same sample

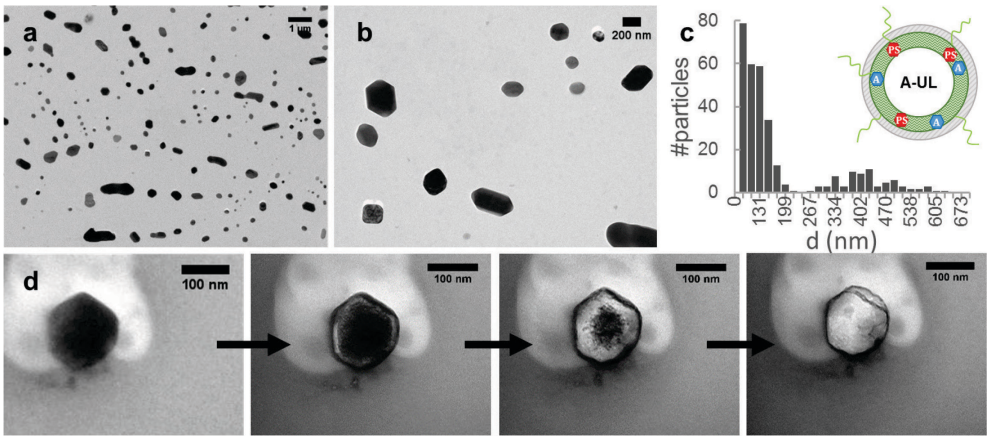

*Figure 7.4. TEM micrographs (a/b) and particle diameter distribution (c, N = 324 particles) of **A-UL**. d) An **A-UL** particle dries out over time during TEM, leaving behind an organosilica shell.*

7.2.2 Preparation of silica-coated liposomes – method A

UL were subsequently used for silica-coating experiments. In the first silica-coating method (method A), **UL** were first coated with (3-aminopropyl)triethoxysilane (APTES) to make organosilica-coated liposomes named **A-UL**, followed by additional coating with pre-hydrolyzed TEOS, making **ApT-UL**. APTES was chosen as initial layer because it has been suggested in the literature that the protonated amino group of APTES (pK_a = 10.4) associates with the negatively charged phospholipid head groups of the liposome membrane;[16d, 16e, 19] in other words, the liposome membrane acts as a template on which APTES hydrolyses and condenses. After the first reaction step and before purification, DLS measurements showed an increase of 20 nm in hydrodynamic size of **A-UL** with respect to **UL** (Table 7.1), suggesting the deposition of an organosilica layer on the membrane of about 10 nm in thickness. As a control, **UL** were kept in the same reaction conditions, without adding APTES. The DLS values of **UL** remained unchanged during these 16 h, which excludes that this change in size was caused by instability of the **UL**. Note that in absence of the liposomes, APTES is likely to form five- or six-membered organosilicate rings in aqueous solution, which suppresses nanoparticle formation.[20] Therefore, APTES alone cannot result in changes in DLS measurements.

To visually confirm the deposition of an APTES layer, **A-UL** were imaged by transmission electron microscopy (TEM), see Figure 7.4. The micrographs show individual particles in various polygonal shapes. No other nanoparticles were observed. Interestingly, when these particles were irradiated by an intense electron beam in the vacuum of the TEM, the liquid inside the particles visibly boiled and leaked out of the particles, leaving behind electron dense shells (Figure 7.4d). This observation suggested that the particles indeed consist of organosilica-coated liposomes. Surprisingly, the particles collapsed only upon high electron irradiation and the particles withstood the high vacuum of the TEM ($\sim 10^{-5}$ bar) at low irradiance, which is evidence that the organosilica layer greatly fortifies the outer shell of a liposome. The average particle diameter from TEM (176 nm, Figure 7.4c) is consistent with the hydrodynamic size observed by DLS (171 nm, Table 7.1). The observed particles with a diameter of around 400 nm are likely to have been individual particles that merged during drying of the TEM grid, because these were absent in DLS measurements. Zeta potentiometry on **A-UL** gave a zeta-potential of −30 mV at *pH* 6.8 (Table 7.1). Such a negative surface charge was

unexpected, given that the amino-groups of the organosilica layer are likely to be protonated at neutral *pH*.

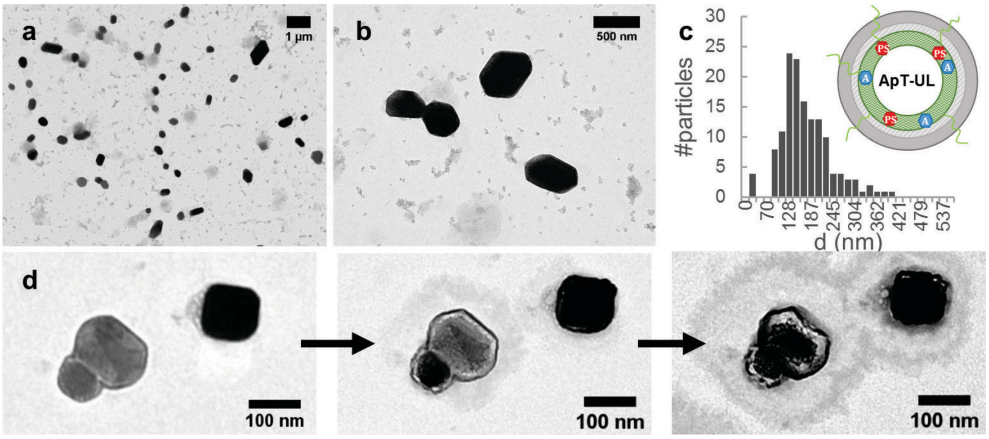

Figure 7.5. TEM micrographs (a/b) and particle diameter distribution (c, N = 142 particles) of ***ApT-UL****. d) An* ***ApT-UL*** *particle dries out over time during TEM, leaving behind an (organo)silica shell.*

The second synthesis step, to make **ApT-UL**, involved coating of **A-UL** with pre-hydrolyzed TEOS, *i.e.* TEOS that had been hydrolyzed for 24 h prior to addition.[17a] This pre-hydrolysis step was found to be essential in acquiring monodispersed silica-coated liposomes: instead of hydrophobic TEOS, that may enter the liposome membrane and disrupt its structure, hydrolyzed TEOS (*i.e.* $Si(OH)_4$ and small condensed oligomers) only condenses in solution. Without pre-hydrolysis the silica-coated liposomes aggregated quickly during the application of the coating. When TEOS was pre-hydrolyzed before addition to **A-UL**, DLS measurement of **ApT-UL** (before washing) showed that the resulting coated liposomes were monodisperse with an increase in hydrodynamic size of 17 nm with respect to the purified **A-UL** (Table 7.1), indicating that an additional layer of silica was deposited on **A-UL**. The DLS values did not change significantly for at least one week after preparation. TEM images showed single particles with an average particle diameter of 163 nm, together with smaller clustered particles, which are probably silica nanoparticles (Figure 7.5). Similar to previous observations with **A-UL**, the particles dried out under intense electron irradiation in the vacuum of the TEM (Figure 7.5d), which allowed direct visualization of the solid silica shell around the liposome. Overall, method A successfully produced (organo)silica-coated liposomes that were mono-dispersed and stable in aqueous solution.

7.2.3 Preparation of silica-coated liposomes – method B

Method B involved the silica-coating of **UL** with TEOS under acidic catalytic conditions to make **T-UL**. Similar methods have previously been used for the silica-coating of micelles.[7a, 7b] Literature suggests that the use of acid catalysis results in more extensive condensation of the silica network,[12b] which might in turn reduce the porosity of the silica layer and improve protection against oxygen. The synthesis method yielded clear solutions that did not aggregate visibly within one week, but an accurate size distribution by DLS could not be obtained (PDI = 1.00). The zeta potential of **T-UL** was found to be negative (−33.4 mV). TEM imaging showed that **T-UL** consists of single dispersed particles with a rather broad size distribution (Figure 7.6). Much smaller particles (< 10 nm) were also present, which are probably silica nanoparticles originating from TEOS condensation in solution instead of on the liposome surface. Interestingly, compared to **A-UL** and **ApT-UL** these particles show only little drying out under intense electron irradiation in the TEM. This may indicate that the silica network in these particles is indeed more condensed than in **A-UL** and **ApT-UL**. Overall, our results demonstrate that using method B resulted in successful silica-coating of liposomes, albeit with a poorly defined particle diameter and poor particle purity.

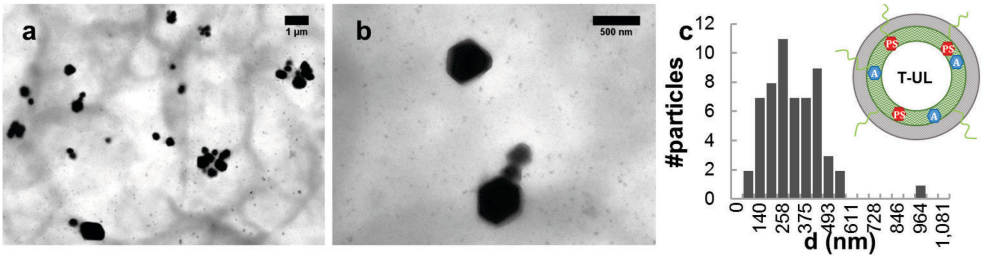

*Figure 7.6. TEM micrographs (a/b) and particle diameter distribution (c, N = 57 particles) of **T-UL**.*

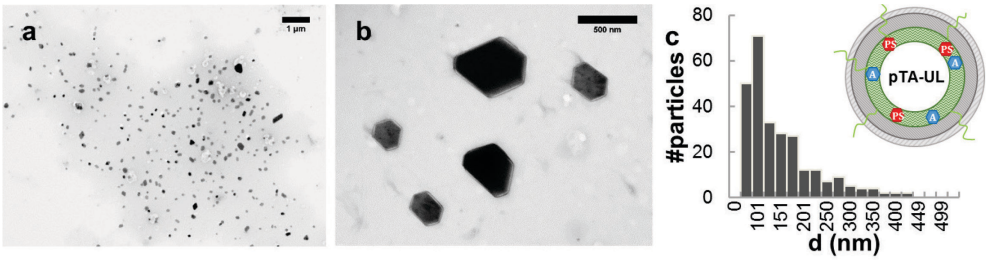

*Figure 7.7. TEM micrographs (a/b) and particle diameter distribution (c, N = 268 particles) of **pTA-UL**.*

7.2.4 Preparation of silica-coated liposomes – method C

Method C involved silica-coating of **UL** with pre-hydrolyzed TEOS to make **pT-UL**, after which the product was additionally coated with APTES to make **pTA-UL**. The zeta-potential of **pT-UL** and **pTA-UL** had similar negative values (−18.8 and −17.0 mV, respectively). Aqueous samples containing **pTA-UL** were not very stable over time; aggregated particles were observed after a few days at room temperature. Freshly prepared **pTA-UL** had an average hydrodynamic size of 167 nm. TEM imaging showed polygonal particles similar to **ApT-UL**, with an average particle diameter of 137 nm. In conclusion, although singly dispersed silica-coated liposomes were produced with method C, the particles were of lower quality than **ApT-UL** from method A in terms of aggregation over time. Overall, these results suggest that an initial APTES "template" layer, such as applied in method A, is beneficial for producing stable silica-coated liposome dispersions.

7.2.5 Spectroscopic properties of silica-coated liposomes in solution

To evaluate whether the silica-coated liposome solutions produced upconversion, samples **A-UL**, **ApT-UL**, **T-UL**, and **PtA-UL** were investigated with UV-vis absorption and emission spectroscopy (λ_{exc} = 630 nm, 10 mW, 80 mW.cm^{-2}), see Figure 7.8. All absorption spectra matched the absorption spectrum of **UL** (Figure 7.3),[1a] which means that the silica-coating did not affect the molecular dyes. Emission spectra were first taken in air, after which sodium sulfite (Na_2SO_3, 50 mM) was added to scavenge ground-state oxygen and the emission spectra were recorded again. Without sulfite, for all solutions only very weak phosphorescence of PdTPTBP (λ_{em} = 800 nm) was observed in comparison with **UL** in presence of sulfite (Figure 7.3). However, upon addition of sulfite, all samples directly exhibited much more intense phosphorescence of PdTPTBP and intense upconverted emission of perylene at 474 nm. In a second experiment, to ascertain that the silica-coating had not destroyed the lipid bilayer, the temperature dependence of phosphorescence and upconversion was recorded between 10 and 35 °C in presence of sulfite (Figure S.VI.1). If the lipid bilayer would still be intact, a steep increase in upconversion and decrease of phosphorescence around the lipid bilayer main transition temperature (T_m ≈ 25 °C) would be expected, just as was observed for **UL** (Figure 7.3). Indeed, in all cases, the thermo-photophysical behavior was similar to **UL**, confirming that the lipid bilayer was still intact. Overall, despite the lipid bilayer being intact inside the particles, it is clear that none of the (organo)silica layers around the liposomes were capable of blocking

oxygen. This must mean that the organo(silica) coating is either porous to oxygen or incomplete, because the capability of upconversion, which takes place inside the particles, is affected by the sodium sulfite added to the solution outside the particles. This result can only be explained if oxygen is able to diffuse freely across the organosilica-coating or across the patches that have remained uncoated.

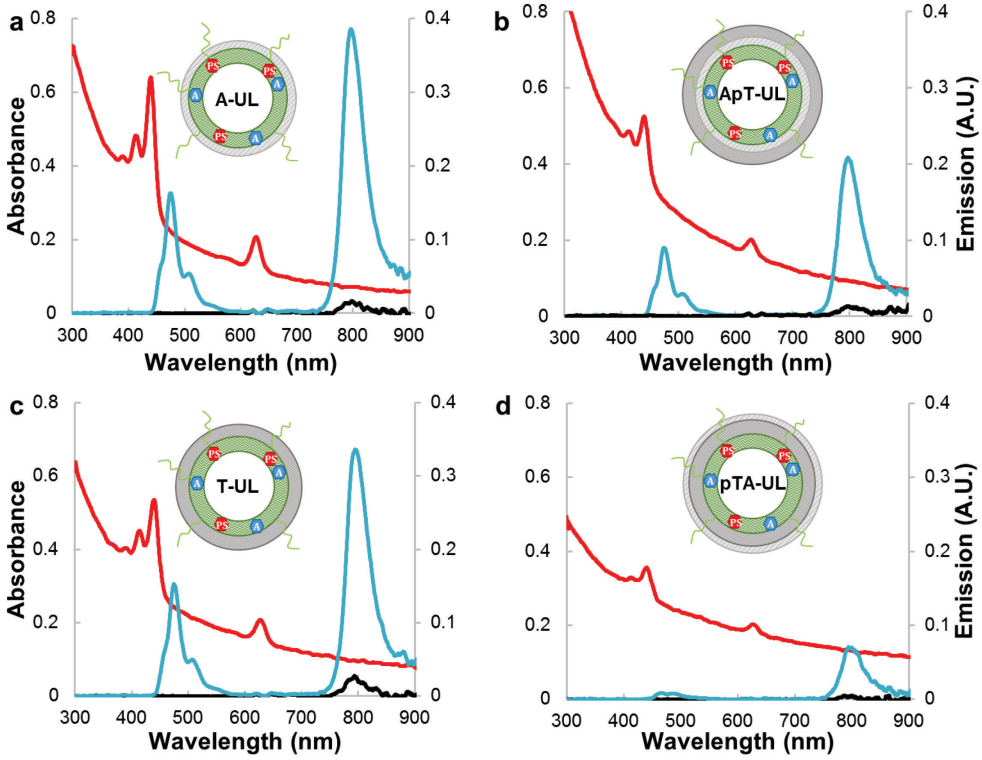

*Figure 7.8. Absorption (red, left axes), and emission spectra in air (black, right axes) and in air in 50 mM Na_2SO_3 PBS (blue, right axes) of **A-UL** (a), **ApT-UL** (b), **T-UL** (c), and **pTA-UL** (d) with 10 mW 630 nm (80 mW.cm^{-2}) at 20 °C.*

Other silica-coated hybrid systems for TTA-UC have been reported. For example, Liu *et al.* described acid-catalyzed silica-coating of TTA-UC dye-loaded Pluronic F-127 micelles with TEOS (similar to method B).[7a, 7b] They showed that the water-soluble particles performed upconversion, but did not mention oxygen quenching of the process at all. In fact, Wang and coworkers used identical particles that were functionalized with two dyes for ratiometric oxygen sensing in cells.[21] Obviously, such particles must be oxygen

permeable if they are used for oxygen sensing. Kwon *et al.* discussed the oxygen sensitivity of an upconverting oleic acid-core silica-shell nanocapsules, with a silica shell thickness of 12 – 23 nm.[5b] While the system was capable of upconversion in air, it was not the relatively thick silica shell that protected the dyes from oxygen, but the oleic acid that is able to scavenge oxygen; without oleic acid, no upconversion was observed. Thus, so far, in all TTA-UC systems with nm-thick silica shells, silica offers no protection from oxygen. Our results seem to be yet another example that nano-size silica layers, made by various methods, is not able to block the diffusion of molecular oxygen in aqueous solution.

7.2.6 Upconversion with silica-coated liposomes in cells

Although TTA-UC in liposomes or (organo)silica-coated liposomes in solution is too oxygen-sensitive, it would be incorrect to assume that they do not function in biological systems. Indeed, TTA-UC has been shown before to occur *in vitro* and *in vivo* with nanoparticle systems that are oxygen sensitive as well.[22] Up to now, a reasonable explanation has not yet been provided in the literature why such particles are able to produce upconversion in biological systems. Possibly, TTA-UC is facilitated by the presence of endogenous anti-oxidants that are able to lower the local oxygen concentration by consuming ground state oxygen or singlet oxygen (see Chapter 8 and Chapter 9). Furthermore, the silica shell may actually offer protection from oxygen in a biological situation in which oxygen is present at a lower concentration than in an aqueous dispersion. With this in mind, A549 lung carcinoma cells were treated with **UL**, **A-UL**, **ApT-UL**, or **pTA-UL** and then imaged with (upconversion) luminescence microscopy. For these experiments, perylene was substituted by 2,5,8,11-tetra(*tert*-butyl)perylene (TBP, Figure 7.1) to prevent the annihilator from escaping the liposomes, which is known to occur for perylene.[23] First of all, uptake of the particles was investigated after 24 h incubation by regular fluorescence microscopy (20x magnification) to image the emission of TBP (λ_{exc} = 377 nm), see Figure S.VI.2. For both liposomes and silica-coated liposomes, the appearance of blue fluorescence throughout the cytosol confirmed the cellular uptake of the particles. The differences in zeta-potential and the presence of the (organo)silica-coating did not seem to affect the particle uptake significantly. Furthermore, no signs of particle toxicity were observed. In a second experiment, the cells were incubated with either **UL** or **ApT-UL** for 24 h and then imaged at 100x magnification with 405 nm and 639 nm excitation under

poorly oxygenated conditions (1% O_2), see Figure 7.9. For both **UL** and **ApT-UL**, under 405 nm excitation, bright fluorescent spots were observed, marking the locations of the TBP dye. Given that the usual uptake mechanism of liposomes is endocytosis, we assign these spots to be endo- and lysosomes. Interestingly, upon 639 nm excitation and observing between 450 to 575 nm, upconverted emission was observed at the same locations as that observed for TBP fluorescence upon 405 nm excitation (Figure 7.9). Comparable upconversion was observed *in vitro* for both **UL** and **ApT-UL**. It was noticed that the upconversion intensity varied significantly from cell to cell, which possibly reflects differences in oxygenation levels and concentration of endogenous anti-oxidants. Overall, **UL** and **ApT-UL** performed upconversion in A549 cells, but silica-coating of the liposomes improved neither uptake nor upconversion luminescence intensity *in vitro*.

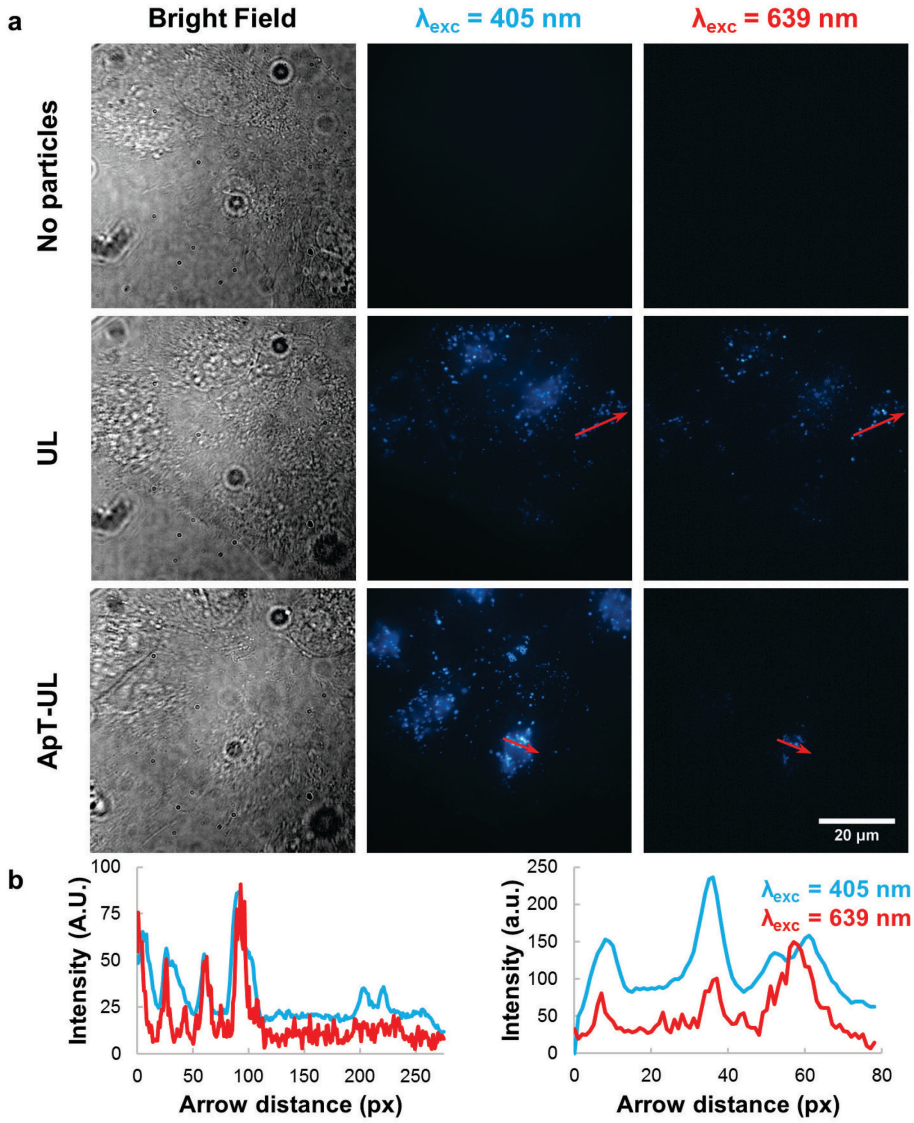

*Figure 7.9. a) Microscopy imaging in bright field mode at 100x magnification and with 405 or 639 nm (26 W.cm^{-2}) excitation of living A549 cells treated with either medium only ("no particles"), **UL**, or **ApT-UL** at 1% O_2, 7% CO_2, and 37 °C. b) Intensity profiles of luminescence observed with 405 and 639 nm along the red arrows given in (a), for samples **UL** (left) and **ApT-UL** (right).*

7.2.7 Dried upconverting silica-coated liposomes

One of the reasons why the silica-coating does not act as an oxygen barrier may be the coating thickness. How thick should the silica-coating be to become a barrier for oxygen? Attempts were undertaken to grow extra layers of silica on **ApT-UL**, but this led inevitably to aggregation of the particles in

solution. As an alternative, it was decided to prepare a solid silica-liposome composite material by drying unpurified **A-UL** and **ApT-UL** samples, *i.e.* without removing the excess of APTES or preTEOS, in an oven at 50 °C overnight. The new samples were called **A-UL-D** and **ApT-UL-D**, respectively. As silica-free control, liposomes **UL** were freeze-dried (sample **UL-F**). For **A-UL-D** and **ApT-UL-D**, heat-drying drives the condensation equilibrium of the (organo)silica network to the fully condensed species by the removal of H_2O and EtOH, making a dense silica material.

The solids were characterized with Scanning Electron Microscopy (SEM) and ^{29}Si-NMR. Figure 7.10 shows SEM images of the solids. **A-UL-D** consisted of a mesh of spherical-polygonal particles within the same size range as the water dispersed **A-UL** particles observed by TEM. The ^{29}Si-NMR spectrum (Figure S.VI.3) shows a broad peak at −68 ppm, corresponding to the fully condensed (T_3) organosilica product of APTES.[20a, 24][II] In comparison, **ApT-UL-D** had a more coarse structure, and individual particles could not be distinguished. This is consistent with the hypothesis that **ApT-UL** particles are embedded in a matrix of amorphous silica. The ^{29}Si-NMR spectrum of this material showed two peaks at −106 and −96 ppm, corresponding to the triple-condensed (Q_3) and double-condensed (Q_2) silica products of TEOS (Figure S.VI.3). Thus, the silica matrix of **ApT-UL-D** is not fully condensed. No signals originating from condensed APTES were detected, which emphasizes that the silica *vs.* organosilica ratio is very high. In contrast, SEM images of **UL-F** suggested that this sticky solid consisted of a network of broken lipid bilayers, which underlines that the silica shell around the liposomes is necessary to conserve the nanostructure of the silica-coated liposomes inside the dried composite materials.

To investigate the integrity of the liposomes inside the material, thermogravimetric analysis (TGA) was performed of all solid samples. If the liposomes would be intact, *i.e.* defined as a lipid bilayer surrounding an aqueous interior, it was expected that first water would escape from ∼100 °C onwards, followed by thermal decomposition of the phospholipids at a higher temperature. Figure 7.11 shows the TGA curves of freeze-dried liposomes **UL-F**, and heat-dried (organo)silica-coated liposomes **A-UL-D** and **ApT-UL-D**. The

[II] ^{29}Si-NMR peak designations are coded by the number of bonded oxygen atoms (T = 3, Q = 4) and by the number of siloxane (Si-O-Si) bonds (subscript 0 – 4).[20a]

mass of **UL-F** reduces by 75% between 230 and 350 °C, indicating the expected thermal decomposition of the phospholipids. The curve for **ApT-UL-D** is very similar to **UL-F**, but with a 40% mass reduction between 230 and 350 °C. The higher residual mass is attributed to the empty residual silica shells, which evidently do not decompose at this temperature. No mass decrease was observed between 30 and 230 °C, indicating the absence of water and thus the absence of intact liposomes inside this material. The TGA curve for **A-UL-D** shows a gradual mass reduction of 13% between 100 and 200 °C, and again a second mass reduction from 230 °C onwards. The mass reductions between 100 and 200 °C suggest the loss of water. However, the theoretical percentage of water mass, assuming 100% synthesis yield and 130 nm diameter liposomes, would amount to 50 – 60%. Therefore, these data indicate that only a relatively small part of **A-UL-D** consist of intact liposomes and that the (organo)silica matrix around the liposomes was not able to prevent drying out of the aqueous interior of the liposomes.

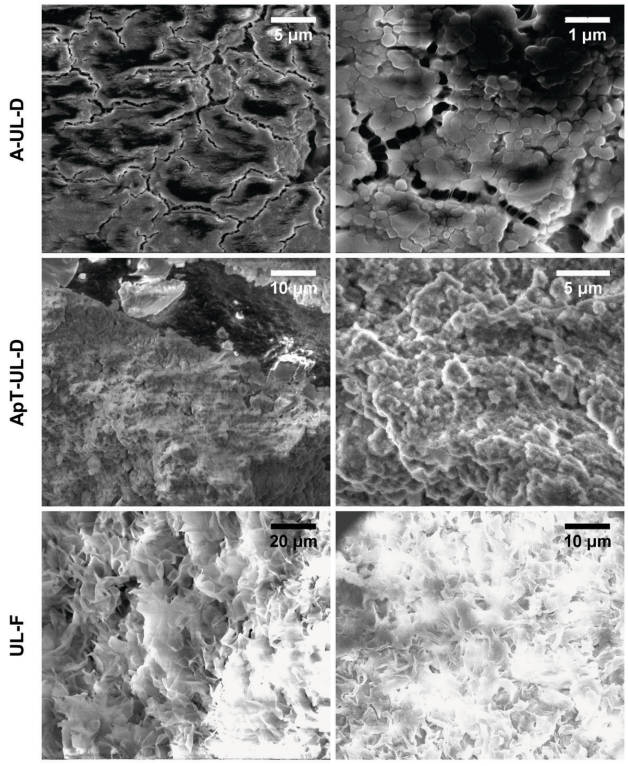

*Figure 7.10. SEM micrographs of dried (organo)silica-coated liposomes **A-UL-D** and **ApT-UL-D**, and freeze-dried liposomes **UL-F**.*

Regardless of the fact that the water inside the material is lost, the residual fragments of dye-doped lipid bilayer inside the solid may still be able to perform upconversion. As an initial test, **A-UL-D** powder was irradiated with 630 nm in air, and surprisingly, blue luminescence was clearly visible after blocking the excitation light (Figure 7.12a). Emission spectroscopy (λ_{exc} = 630 nm, 30 mW, 0.66 W.cm^{-2}) confirmed that **A-UL-D** and **ApT-UL-D** were indeed producing upconverted luminescence under red light irradiation (Figure 7.12b). In contrast, no upconversion in air was detected for freeze-dried liposomes **UL-F** (Figure S.VI.4). These results indicate that (organo)silica can indeed offer protection from oxygen in TTA-UC materials. To offer such protection, however, it is clear that a much thicker layer is necessary than the nano-thick shells applied to water-dispersible silica-coated liposomes. The upconversion emission in **A-UL-D** and **ApT-UL-D** was not very durable; bleaching occurred within minutes at 0.66 W.cm^{-2} irradiance (Figure 7.12c). Time-traces of the upconversion intensity revealed that the emission was more long-lasting for **A-UL-D**. Whereas all upconversion luminescence had bleached within 2 min for **ApT-UL-D**, 40% of the start intensity still remained for **A-UL-D**. This difference may be caused by the greater amount of primary amine groups in **A-UL-D**, which are known to chemically quench singlet oxygen. Such a chemical reaction consumes dioxygen and therefore may contribute to an oxygen-low environment inside the material upon irradiation.[25] Nonetheless, the relative instability of the upconversion emission underlines that even in such bulk materials, (organo)silica does not completely obstruct the diffusion of oxygen. Finally, it must be emphasized that these results are rather preliminary and that the preparation method for obtaining these silica-coated materials can be greatly improved. We foresee that an optimized drying procedure would yield solids with higher degree of silica condensation and in which all the water inside the liposomes remains trapped. Then, the addition of water soluble anti-oxidants to the aqueous interior of the liposomes before silicification and drying, which would end up inside the material, would greatly enhance the upconversion quantum yield and stability in air (see Chapter 8 and Chapter 9). Such highly tunable nano-composite materials, consisting of silica, phospholipids, and water, would effectively allow air-sensitive photophysical processes to take place in a solid state material.

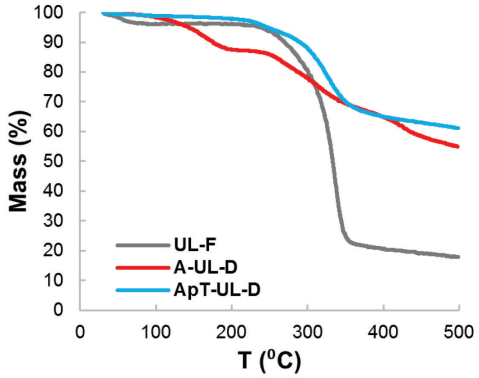

*Figure 7.11. Thermogravimetric analysis plots from 30 to 500 °C (10 °C.min^{-1} in air) of freeze-dried liposomes **UL-F**, and heat-dried (organo)silica-coated liposomes **A-UL-D** and **ApT-UL-D**.*

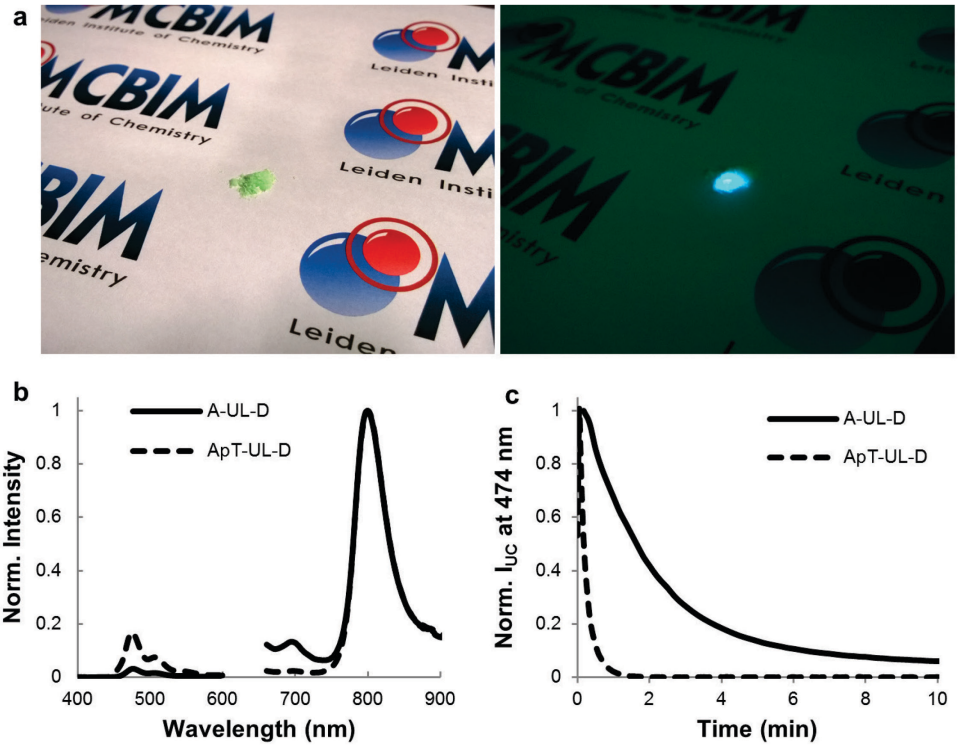

*Figure 7.12. Upconversion with heat-dried silica-coated liposomes. a) Photographs of heat-dried organosilica-coated liposomes **A-UL-D** in ambient light (left) and irradiated with red light and photographed with a 575 nm short pass filter in front of the camera (right). b) Emission spectra of **A-UL-D** (solid) and **ApT-UL-D** (dashed) under 630 nm irradiation, normalized at 800 nm. c) Typical time-traces of the normalized upconversion intensity (I_{UC}) at 474 nm of **A-UL-D** (solid) and **ApT-UL-D** (dashed) under continuous 630 nm irradiation. All experiments were performed at 20 °C with 30 mW 630 nm irradiation (0.66 W.cm^{-2}).*

7.3 Conclusion

Monodisperse (organo)silica-coated liposomes were prepared that can be used to upconvert red light to blue light by means of triplet-triplet annihilation upconversion. The silica-coating did not prevent the upconversion to be quenched by molecular oxygen in solution. Furthermore, the upconverted blue light could be imaged in living A549 cells in hypoxic conditions without causing cytotoxicity, but the luminescence was not more intense than in control cells that had been treated with uncoated upconverting liposomes. However, when the (organo)silica-coated liposomes were heat-dried in presence of excess (organo)silica precursor, solids were obtained that could perform upconversion in air. Our results suggest that the (organo)silica shell of the silica-coated liposomes in solution needs to be much thicker and/or compact to protect the upconversion from oxygen in a biological setting. This work represents noteworthy examples of the combination of phospholipids, water, and silica for the construction of tunable upconverting nanoparticles and materials. Such hybrid systems combine the favorable properties of their constituents, and may eventually be used in applications such as drug delivery, cell imaging, photocatalysis, and solar energy harvesting.

7.4 Experimental Section

7.4.1 General

1,2-dilaureyl-*sn*-glycero-3-phosphocholine (DLPC), 1,2-dimyristoyl-*sn*-glycero-3-phospho choline (DMPC), 1,2-dipalmitoyl-*sn*-glycero-3-phosphocholine (DPPC), and sodium N-(carbonyl-methoxypolyethylene glycol-2000)-1,2-distearoyl-*sn*-glycero-3-phosphoethanolamine (DSPE-mPEG-2000) were purchased from Lipoid GmbH (Ludwigshafen, Germany) and stored at −18 °C. Palladium tetraphenyltetrabenzoporphyrin (PdTPTBP) was purchased from Bio-Connect (Huissen, The Netherlands). Perylene was purchased from Sigma-Aldrich Chemie BV (Zwijndrecht, The Netherlands). The synthesis of 2,5,8,11-tetra(*tert*-butyl)perylene (TBPe) is described in Chapter 9. Dulbecco's phosphate buffered saline (DPBS) was purchased from Sigma Aldrich and had a formulation of 8 $g.L^{-1}$ NaCl, 0.2 $g.L^{-1}$ KCl, 0.2 $g.L^{-1}$ KH_2PO_4, and 1.15 $g.L^{-1}$ K_2HPO_4 with a *pH* of 7.1 − 7.5. All other chemicals were obtained from the major companies and used as received.

7.4.2 Instrumentation

Ultracentrifugation was done with a Beckman-Coulter Optima L-90K ultracentrifuge, equipped with a 70.1 Ti rotor, at 50K rpm (230,000 g) for 30 min. Freeze-dried samples were prepared with a Christ Alpha 1-2 LDPlus machine, operating at <0.03 mbar. Liposome or silica-coated liposome samples were placed in 50 mL round bottom flasks, frozen in liquid nitrogen while gently swirling, and attached to the freeze-dryer. Dynamic Light Scattering (DLS) measurements were performed on undiluted samples ([DMPC] = 10 mM) using a Zetasizer nano

S (Malvern Instruments) operating at 633 nm, with 3 measurements of 12 runs each time. Zeta-potential measurements were performed on a Zetasizer nano ZS (Malvern Instruments), at 25 °C with 3 measurements and 10 − 100 automatic runs. Samples were diluted 20x in MilliQ in a DTS1070 cell, at a known *pH*, so that [DMPC] = 0.5 mM. Fourier Transform Infrared (FT-IR) spectra were recorded on a Perkin-Elmer Paragon 1000. Transmission Electron Microscopy (TEM) imaging was performed on a JEOL 1010 TEM using accelerating voltages of 60.0 or 80.0 kV, iTEM software and a Olympus Megaview G2 camera. Samples were loaded onto Formvar-coated carbon grids (Van Loenen instruments, Netherlands) by depositing a grid on top of a sample droplet for about 30 minutes. CP-MAS ^{29}Si Nuclear Magnetic Resonance (NMR) spectroscopy was performed on a Bruker AV400 using a relaxation delay of 60 seconds and pulse duration of 3 µsec. Scanning Electron Microscopy (SEM) was performed on a Nova NanoSEM (FEI) using accelerating voltages of 15.0 kV. Powder samples were deposited on conducting tape. Thermogravimetric Analysis (TGA) measurements were performed on a Netzsch STA with a DSC/TG Al_2O_3 pan crucible, with a temperature increasing from 30 to 500 °C at 10 °C.min^{-1}, and a gas flow of 40 mL.min^{-1}.

7.4.3 Preparation of upconverting liposomes

Aliquots of stock solutions in chloroform were added together in a round bottom flask to obtain a mixture of DMPC lipid (5 mM in $CHCl_3$, 10 mL, 50 µmol), DSPE-mPEG-2000 (0.2 mM in $CHCl_3$, 10 mL, 2 µmol), PdTPTBP (10 µM in $CHCl_3$, 2.5 mL, 25 nmol) and perylene (0.2 mM in $CHCl_3$, 1.25 mL, 250 nmol). For liposomes used in cell treatment, the perylene dye was replaced by TBPe in the same amount. The solvent was removed by rotary evaporation at 50 °C under reduced pressure and then under high vacuum for at least 15 minutes. PBS buffer (5 mL) was added to the lipid film to obtain a final DMPC lipid concentration of 10 mM. The flask was then freeze-thawed using liquid nitrogen and a water bath at 50 °C for 3 cycles, and the suspension was subsequently extruded using a 200 nm Nuclepore polycarbonate filter and a mini-extruder (Avanti Polar Lipids, Inc.) at 55 °C, for at least 11 times. All dyes were incorporated into the liposomes with minimal losses, as indicated by the lack of color on the filter after the extrusion. The resulting liposome suspension was analyzed by DLS before use in further synthesis steps.

Optionally, an oxygen scavenger was added in a given concentration to the PBS buffer. After extrusion, the oxygen scavenger-loaded liposomes were purified using an Illustra NAP-25 size exclusion column with Sephadex G25 packing (GE Healthcare). Typically, liposomes were loaded on the column in 1 mL portions, and eluted with 2 mL PBS. Fractions of about 0.4 mL were collected; fractions 6 − 10 contained the liposomes as judged by the green-yellow color, fractions 12 and above contained the oxygen scavenger, as judged by the addition of 2,6-dichlorophenolindophenol (DCPIP; 1.0 mM in PBS, 200 µL, 200 nmol) to each fraction. The fractions containing the liposomes (~ 2 mL, *i.e.* [lipid] ≈ 5 mM) were combined and used for further synthesis.

7.4.4 Silica-coating of upconverting liposomes

Silica-coated liposomes were prepared according to a modified literature procedure.[16a, 17a, 17b]

Method A - APTES-preTEOS coating

(3-Aminopropyl)triethoxysilane (APTES, 293 µL, 1.25 mmol) was added to the liposome solution (section 7.4.3, 5 mL, [DMPC] ≈ 5 mM) and the mixture was stirred for 16 h. At this

point, the *pH* was 10.7. To remove unreacted and unassociated APTES, the sample was ultracentrifuged and resuspended in 5 mL PBS twice, which neutralized the *pH*. This washing procedure did not affect the particle size distribution and shape, as judged by TEM (data not shown). Meanwhile, tetraethylorthosilicate (TEOS) was pre-hydrolyzed in PBS (typically 50 mM TEOS) for 24 h at 40 °C, creating a solution of 50 mM pre-hydrolyzed TEOS called "preTEOS". Preliminary experiments determined that a pre-hydrolysis time of 24 hours was optimal for 50 mM TEOS in PBS. A longer time resulted in the formation of non-desired silica nanoparticles (observed by DLS), and a shorter time resulted in sample aggregation during liposome coating. Higher TEOS concentrations resulted in formation of silica nanoparticles as well. Thus, 8 mL preTEOS (50 mM, 400 µmol) was added to the APTES-coated liposome suspension (5 mL) and the mixture was stirred for 24 h at 20 °C. The final APTES-preTEOS coated liposomes were purified by ultracentrifugation and redispersion in 5 mL MilliQ or PBS (once).

Method B – Acid-catalyzed TEOS coating

Liposomes were prepared as mentioned in Section 7.4.3, but instead of PBS, 1 M HCl in PBS was used to hydrate the lipid film. The liposome assembly under such acidic conditions produced high quality liposomes (z-ave 134 nm, 0.1 PDI). After liposome assembly, TEOS (36 µL, 160 µmol) was added to 2 mL of the liposome solution ([DMPC] ≈ 5 mM) and stirred for 30 minutes. Then, the solution was transferred to a dialysis bag (Servapor, MW cutoff 12 – 14 KDa; SERVA Electrophoresis GmbH) and dialyzed against demineralized water (1 L) for 24 h, during which time the water was refreshed twice.

Method C – PreTEOS-APTES coating

First, TEOS was pre-hydrolyzed in PBS (typically 50 mM TEOS) for 24 hours at 40 °C, creating a solution of 50 mM pre-hydrolyzed TEOS called "preTEOS". 8 mL PreTEOS (400 µmol) was then added to the liposome suspension (Section 7.4.3, 5 mL, [DMPC] ≈ 5 mM) and stirred for 24 h at 20 °C. These TEOS-coated liposomes were ultracentrifuged and redispersed in 5 mL PBS twice to remove unreacted and unassociated TEOS. APTES (293 µL, 1.25 mmol) was added to the coated liposome solution (5 mL) and the solution was stirred overnight for 16 h. The final preTEOS-APTES coated liposomes were purified by ultracentrifugation and redispersion in 5 mL MilliQ or PBS (once).

7.4.5 Preparation of (silica-coated) liposome solids

Freeze-dried liposome solids were prepared by freeze-drying at ≤ 0.03 mbar (section 7.4.2). Oven-dried silica-coated liposome solids were prepared by depositing unpurified silica-coated liposomes **A-UL** or **ApT-UL** (*i.e.* including excess APTES and/or preTEOS) in 5 mL portions on watch glasses and drying overnight at 50 °C.

7.4.6 UV-Vis absorption and emission spectroscopy

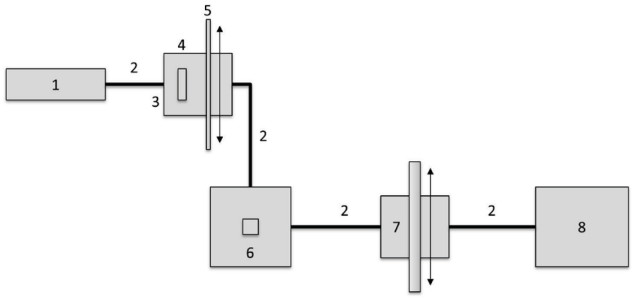

Figure 7.13 Setup used for emission spectroscopy on samples in solution using red light irradiation. Legend: (1) 630 nm laser source, (2) optical fibers, (3) filter holder, (4) 630 nm band pass filter, (5) variable neutral density filter, (6) temperature controlled cuvette holder, (7) variable filter holder with a 633 nm notch filter, and (8) CCD spectrometer.

Absorption and emission spectroscopy was performed with a custom-built setup (Figure 7.13). Typically, a 2 mL sample was transferred in a 111-OS macro fluorescence cuvette from Hellma and placed in a CUV-UV/VIS-TC temperature-controlled cuvette holder from Avantes (Apeldoorn, The Netherlands). Every time the temperature was changed, the sample was allowed to equilibrate for 5 minutes. The samples were irradiated from the side with a 10 mW 630 nm laser light beam from a clinical grade Diomed 630 nm PDT laser (4 mm beam, 80 $mW.cm^{-2}$). The 630 nm light was filtered through a FB630-10, 630 nm band pass filter (Thorlabs, Dachau/Munich, Germany) put between the laser and the sample. The excitation power was controlled using a NDL-25C-4 variable neutral density filter (Thorlabs), and measured using a S310C thermal sensor connected to a PM100USB power meter (Thorlabs). An Avantes 2048L StarLine CCD spectrometer was connected at 90° angle with respect to the excitation source. A Thorlabs NF-633 notch filter placed between the cuvette holder and the spectrometer was used to block the excitation light. To make the emission spectra of the different samples in solution comparable, the samples were diluted in PBS so that A_{630} = 0.20. Optionally, Na_2SO_3 (1 mL, 100 mM in PBS, pH = 7.4) was freshly added to 1 mL samples so that 50 mM Na_2SO_3 was present for oxygen scavenging during spectroscopy.

7.4.7 Solid state emission spectroscopy

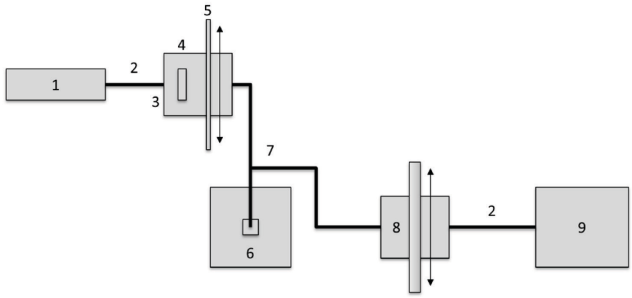

Figure 7.14. Setup used for emission spectroscopy on powders using red light irradiation. Legend: (1) 630 nm laser source, (2) optical fibers, (3) filter holder, (4) 630 nm band pass filter, (5) variable neutral density filter, (6) temperature controlled cuvette holder, (7) bifurcated optical fiber, (8) variable filter holder with a 633 nm notch filter, and (9) CCD spectrometer.

Solid state emission spectroscopy was done in a slightly different setup than for liquid samples (Figure 7.14). A bifurcated fiber (FCB UVIR 400-2, Avantes) was connected to the top of the cuvette holder, in which a lens (Avantes COL-UV/VIS lens, f = 8.7 mm) was fitted that simultaneously transmitted excitation light and captured the emission. 7.1 mg solid sample was deposited on the bottom of a semi-micro cuvette. Samples were irradiated with 30 mW 630 nm light (2.4 mm beam, 0.66 $W.cm^{-2}$).

7.4.8 General cell culturing

A549 human lung carcinoma cells were cultured in 25 cm^2 flasks in 8 mL Dulbecco's Modified Eagle Medium with phenol red (DMEM; Sigma Life Science, USA), supplemented with 8.2% v/v fetal calf serum (FCS; Hyclone), 200 $mg.L^{-1}$ penicillin and streptomycin (P/S; Duchefa), and 1.8 mM glutamine S (GM; Gibco, USA), under standard culturing conditions (humidified, 37 °C atmosphere containing 7.0% CO2). The cells were split approximately once per week upon reaching 70 − 80% confluency, using seeding densities of 2×10^5 cells, and the medium was refreshed once per week. Cells were passaged for 4 − 8 weeks.

7.4.9 Regular fluorescence microscopy

For regular fluorescence microscopy experiments, cells were seeded into 6-well plates, 200K cells per well. Meanwhile, the liposome- or silica-coated liposome-samples at a 2.5 mM lipid concentration were filtered through a 0.45 µm filter and further brought to a 1 mM final lipid concentration with OptiMEM (Life Technologies, USA), supplemented with 2.5% FCS, 200 mg/L P/S, and 1.8 mM GM ("OptiMEM complete"). 24 h after cell seeding, 3 mL of liposome mixture was added to each well, and the cells were incubated for another 24 hours. Then, the liposomes were removed and the cells were washed once with PBS and supplied with 1 mL OptiMEM. The cells were imaged in bright field mode (250 ms exposure) and with 377 nm excitation (1000 ms exposure) using a Leica SPE confocal microscope at 20x magnification and Cell^M software.

7.4.10 Upconversion luminescence microscopy

For upconversion microscopy experiments, cells were seeded at 30K on 25 mm diameter microscopy coverslips (VWR, thickness no. 1) in 6-well plates. Meanwhile, the liposome- or silica-coated liposome-samples at a 2.5 mM lipid concentration were filtered through a 0.45 µm pore filter and further brought to a 1 mM final lipid concentration with OptiMEM complete. 24 h after seeding, 3 mL liposome-medium mixture was added to each well and incubated for 24 h. Then, the liposomes were washed once with PBS and supplied with 1 mL OptiMEM. The coverslips were transferred to custom-made coverslip holders, which in turn were put in a stage-top miniature incubator (Tokai Hit, INUBG2ETFP-WSKM) fitted with a GM-8000 gas controller. The cells were incubated for 30 minutes at 1% O_2, 7% CO_2, and 37 °C before imaging. Imaging was performed with a customized Zeiss Axiovert S100 Inverted Microscope setup, fitted with a Zeiss 100x Plan Apochromat 1.4 NA oil objective, and an Orca Flash 4.0 V2 sCMOS camera from Hamamatsu, which together produced images with pixel size of 69 nm (for 100x). The typical camera exposure time was 1000 ms. Excitation at 405 nm was performed with a CrystaLaser DL405-050 diode laser, in combination with a Chroma zet442/514/568m emission filter and Chroma zt405/514/561rpc dichroic mirror. The output power of the 405 nm laser at the sample was typically 62 µW at 100 x magnification (60 µm spot diameter, intensity 2.2 $W.cm^{-2}$). Excitation at 639 nm was performed with a Power Technology 1Q1A30(639-35B)G3 diode laser, in combination with a 575 nm short pass filter (Edmund Optics, part no. #84-709) and Chroma zt405/532/635rpc dichroic mirror. The output power of the 639 nm laser at the

sample was typically 1.0 mW at 100 x magnification (70 µm spot diameter, 26 $W.cm^{-2}$ intensity).

7.5 References

[1] a) S. H. C. Askes, A. Bahreman, S. Bonnet, *Angew. Chem., Int. Ed.* **2014**, *53*, 1029-1033; b) S. H. C. Askes, M. Kloz, G. Bruylants, J. T. Kennis, S. Bonnet, *Phys. Chem. Chem. Phys.* **2015**, *17*, 27380-27390; c) Z. Chen, W. Sun, H.-J. Butt, S. Wu, *Chem. Eur. J.* **2015**, *21*, 9165-9170; d) J. Zhou, Q. Liu, W. Feng, Y. Sun, F. Li, *Chem. Rev.* **2014**, *115*, 395-465; e) L. Xia, X. Kong, X. Liu, L. Tu, Y. Zhang, Y. Chang, K. Liu, D. Shen, H. Zhao, H. Zhang, *Biomaterials* **2014**, *35*, 4146-4156; f) E. Ruggiero, J. Hernandez-Gil, J. C. Mareque-Rivas, L. Salassa, *Chem. Commun.* **2015**.

[2] a) T. N. Singh-Rachford, F. N. Castellano, *Coord. Chem. Rev.* **2010**, *254*, 2560-2573; b) T. W. Schmidt, F. N. Castellano, *J. Phys. Chem. Lett.* **2014**, *5*, 4062-4072; c) A. Monguzzi, R. Tubino, S. Hoseinkhani, M. Campione, F. Meinardi, *Phys. Chem. Chem. Phys.* **2012**, *14*, 4322-4332; d) N. Yanai, N. Kimizuka, *Chem. Commun.* **2016**, *52*, 5354-5370.

[3] a) S. Hisamitsu, N. Yanai, N. Kimizuka, *Angew. Chem. Int. Ed.* **2015**, *54*, 11550-11554; b) P. Mahato, A. Monguzzi, N. Yanai, T. Yamada, N. Kimizuka, *Nat. Mater.* **2015**, *14*, 924-930; c) S. H. Lee, D. C. Thévenaz, C. Weder, Y. C. Simon, *J. Polym. Sci., Part A: Polym. Chem.* **2015**, *53*, 1629-1639; d) P. Duan, N. Yanai, H. Nagatomi, N. Kimizuka, *J. Am. Chem. Soc.* **2015**, *137*, 1887-1894; e) P. Duan, N. Yanai, N. Kimizuka, *J. Am. Chem. Soc.* **2013**, *135*, 19056–19059; f) A. J. Svagan, D. Busko, Y. Avlasevich, G. Glasser, S. Baluschev, K. Landfester, *ACS Nano* **2014**, *8*, 8198-8207.

[4] a) J.-H. Kim, J.-H. Kim, *ACS Photonics* **2015**, *2*, 633-638; b) Z. Huang, X. Li, M. Mahboub, K. Hanson, V. Nichols, H. Le, M. L. Tang, C. J. Bardeen, *Nano Lett.* **2015**, *15*, 5552-5557.

[5] a) M. Majek, U. Faltermeier, B. Dick, R. Pérez-Ruiz, A. Jacobi von Wangelin, *Chem. Eur. J.* **2015**, *21*, 15496-15501; b) O. S. Kwon, J. H. Kim, J. K. Cho, J. H. Kim, *ACS Appl. Mater. Interfaces* **2015**, *7*, 318-325.

[6] a) A. Monguzzi, S. M. Borisov, J. Pedrini, I. Klimant, M. Salvalaggio, P. Biagini, F. Melchiorre, C. Lelii, F. Meinardi, *Adv. Funct. Mater.* **2015**, *25*, 5617-5624; b) A. Nattestad, C. Simpson, T. Clarke, R. W. MacQueen, Y. Y. Cheng, A. Trevitt, A. J. Mozer, P. Wagner, T. W. Schmidt, *Phys. Chem. Chem. Phys.* **2015**; c) S. P. Hill, T. Banerjee, T. Dilbeck, K. Hanson, *J. Phys. Chem. Lett.* **2015**, *6*, 4510-4517; d) A. Nattestad, Y. Y. Cheng, R. W. MacQueen, T. F. Schulze, F. W. Thompson, A. J. Mozer, B. Fückel, T. Khoury, M. J. Crossley, K. Lips, G. G. Wallace, T. W. Schmidt, *J. Phys. Chem. Lett.* **2013**, *4*, 2073-2078.

[7] a) Q. Liu, W. Feng, T. Yang, T. Yi, F. Li, *Nat. Protocols* **2013**, *8*, 2033-2044; b) Q. Liu, T. Yang, W. Feng, F. Li, *J. Am. Chem. Soc.* **2012**, *134*, 5390-5397; c) A. Nagai, J. B. Miller, P. Kos, S. Elkassih, H. Xiong, D. J. Siegwart, *ACS Biomater. Sci. Eng.* **2015**, *1*, 1206-1210; d) C. Wohnhaas, V. Mailänder, M. Dröge, M. A. Filatov, D. Busko, Y. Avlasevich, S. Baluschev, T. Miteva, K. Landfester, A. Turshatov, *Macromol. Biosci.* **2013**, *13*, 1422–1430; e) C. Wohnhaas, A. Turshatov, V. Mailänder, S. Lorenz, S. Baluschev, T. Miteva, K. Landfester, *Macromol. Biosci.* **2011**, *11*, 772-778; f) Q. Liu, B. Yin, T. Yang, Y. Yang, Z. Shen, P. Yao, F. Li, *J. Am. Chem. Soc.* **2013**, *135*, 5029-5037; g) O. S. Kwon, H. S. Song, J. Conde, H.-i. Kim, N. Artzi, J.-H. Kim, *ACS Nano* **2016**, *10*, 1512-1521.

[8] a) R. R. Sawant, V. P. Torchilin, *Soft Matter* **2010**, *6*, 4026-4044; b) A. S. L. Derycke, P. A. M. de Witte, *Adv. Drug Delivery Rev.* **2004**, *56*, 17-30; c) T. M. Allen, P. R. Cullis, *Adv. Drug Delivery Rev.* **2012**.

[9] a) H. J. Feldmann, M. Molls, P. Vaupel, *Strahlenther. Onkol.* **1999**, *175*, 1-9; b) P. Vaupel, F. Kallinowski, P. Okunieff, *Cancer Res.* **1989**, *49*, 6449-6465; c) E. E. Graves, M. Vilalta, I. K. Cecic, J. T. Erler, P. T. Tran, D. Felsher, L. Sayles, A. Sweet-Cordero, Q.-T. Le, A. J. Giaccia, *Clin. Cancer Res.* **2010**, *16*, 4843-4852.

[10] C. Wohnhaas, K. Friedemann, D. Busko, K. Landfester, S. Baluschev, D. Crespy, A. Turshatov, *ACS Macro Lett.* **2013**, *2*, 446-450.

[11] F. Marsico, A. Turshatov, R. Peköz, Y. Avlasevich, M. Wagner, K. Weber, D. Donadio, K. Landfester, S. Baluschev, F. R. Wurm, *J. Am. Chem. Soc.* **2014**.

[12] a) C. J. Brinker, G. W. Scherer, *Sol-Gel Science: The Physics And Chemistry Of Sol-Gel Processing*, Academic Press, Inc., **1990**; b) C. J. Brinker, *J. Non-Cryst. Solids* **1988**, *100*, 31-50; c) C. Barbe, J. Bartlett, L. G. Kong, K. Finnie, H. Q. Lin, M. Larkin, S. Calleja, A. Bush, G. Calleja, *Adv. Mater.* **2004**, *16*, 1959-1966; d) S. S. Lucky, K. S. Soo, Y. Zhang, *Chem. Rev.* **2015**.

[13] M. Frasconi, Z. C. Liu, J. Y. Lei, Y. L. Wu, E. Strekalova, D. Malin, M. W. Ambrogio, X. Q. Chen, Y. Y. Botros, V. L. Cryns, J. P. Sauvage, J. F. Stoddart, *J. Am. Chem. Soc.* **2013**, *135*, 11603-11613.

[14] Y. Leterrier, *Prog. Mater Sci.* **2003**, *48*, 1-55.

[15] a) M. Mirenda, V. Levi, M. L. Bossi, L. Bruno, A. V. Bordoni, A. E. Regazzoni, A. Wolosiuk, *J. Colloid Interface Sci.* **2013**, *392*, 96-101; b) D. Zhang, Z. Wu, J. Xu, J. Liang, J. Li, W. Yang, *Langmuir* **2010**, *26*, 6657-6662; c) L. M. Rossi, L. Shi, F. H. Quina, Z. Rosenzweig, *Langmuir* **2005**, *21*, 4277-4280.

[16] a) N. Folliet, C. Roiland, S. Bégu, A. Aubert, T. Mineva, A. Goursot, K. Selvaraj, L. Duma, F. Tielens, F. Mauri, G. Laurent, C. Bonhomme, C. Gervais, F. Babonneau, T. Azaïs, *J. Am. Chem. Soc.* **2011**, *133*, 16815-16827; b) S. Begu, R. Durand, D. A. Lerner, C. Charnay, C. Tourne-Peteilh, J. M. Devoisselle, *Chem. Commun.* **2003**, 640-641; c) D. H. W. Hubert, M. Jung, P. M. Frederik, P. H. H. Bomans, J. Meuldijk, A. L. German, *Adv. Mater.* **2000**, *12*, 1286-1290; d) N. V. Beloglazova, O. A. Goryacheva, E. S. Speranskaya, T. Aubert, P. S. Shmelin, V. R. Kurbangaleev, I. Y. Goryacheva, S. De Saeger, *Talanta* **2015**, *134*, 120-125; e) N. V. Beloglazova, I. Y. Goryacheva, P. S. Shmelin, V. Kurbangaleev, S. De Saeger, *J. Mater. Chem. B* **2015**, *3*, 180-183; f) A. Corma, U. Díaz, M. Arrica, E. Fernández, Í. Ortega, *Angew. Chem., Int. Ed.* **2009**, *48*, 6247-6250; g) S. Shen, L. Yang, Y. Lu, J.-G. Chen, S. Song, D. Hu, A. Parikh, *ACS Appl. Mater. Interfaces* **2015**.

[17] a) S. Bégu, A. A. Pouëssel, D. A. Lerner, C. Tourné-Péteilh, J. M. Devoisselle, *J. Controlled Release* **2007**, *118*, 1-6; b) S. Begu, S. Girod, D. A. Lerner, N. Jardiller, C. Tourne-Peteilh, J. M. Devoisselle, *J. Mater. Chem.* **2004**, *14*, 1316-1320; c) Y. Steinberg, A. Schroeder, Y. Talmon, J. Schmidt, R. L. Khalfin, Y. Cohen, J.-M. Devoisselle, S. Begu, D. Avnir, *Langmuir* **2007**, *23*, 12024-12031.

[18] D. Marsh, *Handbook of Lipid Bilayers*, 2nd ed., Taylor & Francis Group, LLC, Boca Raton, FL, USA, **2013**.

[19] F. Wang, S. L. Nimmo, B. Cao, C. Mao, *Chem. Sci.* **2012**, *3*, 2639-2645.

[20] a) S. Chen, S. Hayakawa, Y. Shirosaki, E. Fujii, K. Kawabata, K. Tsuru, A. Osaka, *J. Am. Ceram. Soc.* **2009**, *92*, 2074-2082; b) A. van Blaaderen, A. Vrij, *J. Colloid Interface Sci.* **1993**, *156*, 1-18.

[21] X.-d. Wang, J. A. Stolwijk, T. Lang, M. Sperber, R. J. Meier, J. Wegener, O. S. Wolfbeis, *J. Am. Chem. Soc.* **2012**, *134*, 17011-17014.

[22] a) Q. Liu, T. S. Yang, W. Feng, F. Y. Li, *J. Am. Chem. Soc.* **2012**, *134*, 5390-5397; b) C. Wohnhaas, V. Mailander, M. Droge, M. A. Filatov, D. Busko, Y. Avlasevich, S. Baluschev, T. Miteva, K. Landfester, A. Turshatov, *Macromol. Biosci.* **2013**, *13*, 1422-1430.

[23] M. Almgren, *J. Am. Chem. Soc.* **1980**, *102*, 7882-7887.

[24] S. H. Kim, O. H. Han, J. K. Kim, K. H. Lee, *Bull. Korean Chem. Soc.* **2011**, *32*, 3644-3649.

[25] a) B. Rånby, J. F. Rabek, *Singlet Oxygen Reactions with Organic Compounds & Polymers*, John Wiley & Sons, Ltd., **1978**; b) F. A. Carey, R. J. Sundberg, *Advanced Organic Chemistry*, 5 ed., Springer US, **2007**.